Biochimica et Biophysica Acta 1777 (2008) 1032–1037

Contents lists available at ScienceDirect

Biochimica et Biophysica Acta

journal homepage: www.elsevier.com/locate/bbabio

Distance metrics for heme protein electron tunneling

Christopher C. Moser *, Sarah E. Chobot, Christopher C. Page, P. Leslie Dutton

Johnson Research Foundation, Department of Biochemistry and Biophysics, University of Pennsylvania, Philadelphia, PA 19104, USA

ARTICLE INFO

Article history:
Received 1 February 2008
Received in revised form 17 March 2008
Accepted 13 April 2008
Available online 18 April 2008

Keywords:
Protein electron tunneling
Heme
Ruthenium
Electron transfer

ABSTRACT

There is no doubt that distance is the principal parameter that sets the order of magnitude for electron-tunneling rates in proteins. However, there continue to be varying ways to measure electron-tunneling distances in proteins. This distance uncertainty blurs the issue of whether the intervening protein medium has been naturally selected to speed or slow any particular electron-tunneling reaction. For redox cofactors lacking metals, an edge of the cofactor can be defined that approximates the extent in space that includes most of the wavefunction associated with its tunneling electron. Beyond this edge, the wavefunction tails off much more dramatically in space. The conjugated porphyrin ring seems a reasonable edge for the metal-free pheophytins and bacteriopheophytins of photosynthesis. For a metal containing redox cofactor such as heme, an appropriate cofactor edge is more ambiguous. Electron-tunneling distance may be measured from the conjugated heme macrocycle edge or from the metal, which can be up to 4.8 Å longer. In a typical protein medium, such a distance difference normally corresponds to a ~1000 fold decrease in tunneling rate. To address this ambiguity, we consider both natural heme protein electron transfer and light-activated electron transfer in ruthenated heme proteins. We find that the edge of the conjugated heme macrocycle provides a reliable and useful tunneling distance definition consistent with other biological electron-tunneling reactions. Furthermore, with this distance metric, heme axially- and edge-oriented electron transfers appear similar and equally well described by a simple square barrier tunneling model. This is in contrast to recent reports for metal-to-metal metrics that require exceptionally poor donor/acceptor couplings to explain heme axially-oriented electron transfers.

1. Introduction

1.1. Typical intraprotein electron-tunneling rates

Electron-tunneling reactions in natural proteins span nearly 12 orders of magnitude in time and distances from 4 to 24 Å. Nature has selected distances at the short end of this range, from about 4 to 14 Å, to maintain productive electron-tunneling reactions at a rate faster than the commonly observed millisecond catalytic turnover times of natural proteins[1]. Longer distances are associated with short-circuit reactions that can be observed under certain circumstances. Besides distance (R), electron-tunneling rates also depend on the driving force of electron transfer (ΔG°). Marcus[2] described the behavior seen in many tunneling systems in which the electron-tunneling rate has a Gaussian dependence on driving force, increasing from low driving force to a maximum rate when the driving force matches a parameter called the reorganization energy (λ), and then falling again as the driving force is increased beyond the optimum. In biological systems, it appears there are often vibrational energies associated with the electron tunneling between donor and acceptor which are larger than ambient thermal energies[3]. This leads to a free energy dependence of the tunneling rate on driving force which has some quantum character inconsistent with the classical Marcus description. This slightly broadens the Gaussian dependence of tunneling rate on driving force. A plot of the free energy optimized electron-tunneling rate as a function of the distance between the edges of the various photosynthetic redox cofactors of both purple bacteria[4] and photosystem I (PSI)[5,6] (Fig. 1A) shows a nearly exponential relationship between rate and distance, with an optimal tunneling rate at closest distances of about 10^{13} s^{-1} (near the maximum Eyring rate of transition state theory) and falling off by an order of magnitude for every 1.7 Å. Such simple exponential distance decay is expected for tunneling through an effectively uniform insulating protein barrier, a "square barrier". A simple empirical expression that captures this exponential distance dependence and Gaussian free energy dependence, using units of Å for distance and eV for ΔG° and λ is s follows[4].

$$\text{Log}\ k_{et} = 15 - 0.6R - 3.1\left(\left(\Delta G^{o} + \lambda\right)^{2}\right)/\lambda \quad (1)$$

This expression is adequate for predicting electron-tunneling rates in many biological systems to within an order of magnitude. Better accuracy than this is hard to achieve, principally because of uncertainty

* Corresponding author. 1005 Stellar-Chance Laboratories Department of Biochemistry and Biophysics University of Pennsylvania, Philadelphia, PA 19104-6059, USA. Tel.: +1 215 573 3909; fax: +1 215 573 2235.
E-mail address: moserc@mail.med.upenn.edu (C.C. Moser).

0005-2728/$ – see front matter © 2008 Elsevier B.V. All rights reserved.
doi:10.1016/j.bbabio.2008.04.021

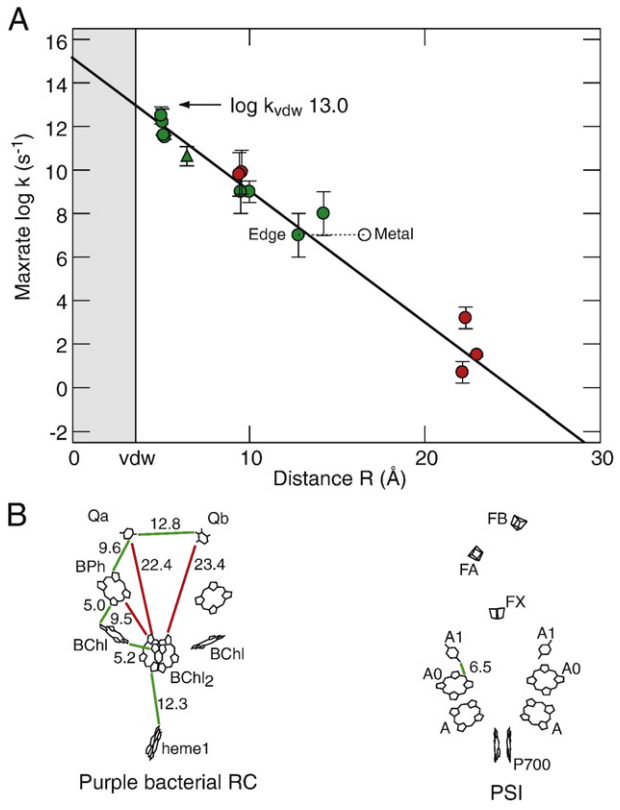

Fig. 1. A) Optimal rates of electron tunneling between cofactors with reorganization energy estimates in purple bacterial reaction centers and PSI. Productive electron transfers, green; unproductive charge recombinations, red. For the heme to $BChl_2$ reaction edge- and metal-centered distance metrics are noted. B) Reaction center (RC) structures from PDB files 1PRC[35] and 1JBO[36].

in the three principle parameters: driving force, reorganization energy, and distance. Driving forces are usually estimated from the relative redox potentials of the donor and acceptor, which may not be available. Reorganization energy is best defined by analyzing the free energy dependence of the electron-tunneling rate. Typically the redox potentials of the cofactors are changed via mutation or chemical substitution and fit to a Gaussian curve to find the free energy that provides the fastest tunneling rates. When a free energy dependence is not known, best guesses for the reorganization energy will be ~0.7 ± 0.5 eV; this value is lower for reactions in which donor and acceptor are large and buried in a hydrophobic environment, and higher for more compact cofactors in hydrophilic environments. The simpler method of estimating the reorganization energy from the temperature dependence of the reaction assumes a classical Marcus description, which we have seen to be inappropriate for some of the best studied systems[3]. Temperature changes can also introduce driving force changes and dynamic effects not directly related to the tunneling event. Protein crystal structures can in principle provide estimates of the distance parameter, but this assumes not only that the protein is not dynamic with noticeable changes in distance between donor and acceptor, but also that it is clear how to derive the appropriate tunneling distance from the structure in the first place, a topic we will address here. Some donors and acceptors have relatively compact wavefunctions for the tunneling electrons that are highly localized on an individual metal atom, so that the barrier through which the electron must tunnel includes both non-metal atoms of the cofactor as well as the insulating protein medium between donor and acceptor. In other cases, especially in photosynthetic systems, it is clear that the tunneling electron wavefunction is considerably delocalized and the "edge" of the tunneling barrier should extend to include the conjugated atoms of the cofactor[7].

In principle, the insulating protein medium between donor and acceptor could have been selected by Nature to accelerate or decelerate any particular electron-tunneling reaction. This is because the more covalently linked the medium between donor and acceptor, the lower the electron-tunneling barrier tends to appear, and the faster the rate of electron tunneling. Direct, covalent links between donor and acceptor tend to have the fastest tunneling rates for any given distance, as seen in a number of chemically constructed systems [4]. Measures of the linked quality of the protein insulation between donor and acceptor use algorithms of varying complexity. One approach finds the best linkage combinations of covalent bonds and through space gaps, considering possible quantum interference and dynamical effects[8,9], while another provides a simple estimate of the packing density of the protein medium as a proxy for the effective barrier height[1]. However, direct covalent links between donor and acceptor are rarely achieved in a natural protein system. Furthermore, there seems to be no evidence that natural selection has acted on the protein medium to modulate the rate of electron tunneling, either by lowering the barrier for useful reactions or raising the barrier for non-useful reactions. This is illustrated clearly in Fig. 1A, which shows that both productive charge separating reactions (green) and unproductive charge recombination reactions (red) in photosynthesis have the same general distance/rate dependence. Thus, it appears that even the simple expression of Eq. (1), which is a protein medium independent, square barrier tunneling model, provides an adequate means to estimate natural intraprotein electron-transfer rates within the experimental error.

Fig. 1 shows that within the uncertainty of experimental measurement of tunneling rate, driving force and reorganization energy, and seemingly minor variations in the tunneling barrier presented by protein in biological electron transfers, tunneling distances with chlorins can be consistently and appropriately measured from the conjugated macrocycle edge, while tunneling distances for quinones can be from the ring atoms and attached oxygens[7]. However, it is less clear how to define the edge of the heme cofactors, as there is only one example of a photosynthetic reaction with a driving force derived measure of the reorganization energy, namely heme to the bacteriochlorophyll dimer, $BChl_2$. Because in this case the heme has a nearly edge-on orientation towards the $BChl_2$ (Fig. 1B), there is a substantial difference in distance and expected rates for either a macrocycle edge or metal center tunneling distance. In this case, the macrocycle edge definition is much more in line with the tunneling rates in other photosynthetic reactions (Fig. 1A).

1.2. Distance dependence in ruthenated heme proteins

We can expand this thin natural heme reaction data set to include unnatural electron-tunneling reactions for which reorganization energy determinations have been made, allowing reliable estimates of the optimal electron-tunneling rate. Four heme proteins, myoglobin [10,11] and cytochromes *c*[11–18], b_5[19,20], and b_{562}[16], have been chemically modified to include a light-activatable ruthenium (Ru) label, and electron-transfer rates back and forth between the heme and Ru centers have been measured. Conveniently, the lifetimes of the photogenerated ruthenium centers coupled with the driving forces of the electron-tunneling reactions yield electron-tunneling distances that tend to be over the ~10 Å range between those of the shorter, productive and longer, unproductive natural electron transfers[21].

The distance dependence of the free energy optimized rate of electron tunneling in these ruthenated heme proteins can be presented using two distinct distance metrics: metal-to-metal (Ru–Fe) or Ru-to-heme macrocycle. An unavoidable complication in such data sets is the possibility for considerable mobility of the ruthenium cofactors, unlike the cofactors in the natural photosystems. This mobility can be small for buried Ru centers, or rather large for some

surface labels. In the absence of a crystal structure for each label, one way to estimate tunneling distances is to perform an energy minimization of a model of the structure, as might be appropriate if the motion of the label was slow on the timescale of the measurement. This has been done for the metal-to-metal distance metric (gray in Fig. 2)[16]. On the other hand, given the general observation that the distance dependence of the tunneling rate is roughly exponential, closer approaches of the two centers may be weighed more heavily in the effective tunneling distance, especially if motion of the label is fast on the timescale of the measurement. This has been done for the metal-to-heme distance metric in which the plotted distance represents a model of the closest approach of the Ru center to the heme that does not result in overlap of the Ru label with residues in the unlabeled protein crystal structure (blue in Fig. 2). Fig. 2 also includes for comparison the Ru-to-metal or Ru-to-edge distances for ruthenated proteins azurin[10,22,23], and HiPIP[24].

The log rate vs. distance slopes for both of these metrics are roughly similar, although the heme-edge metric of course has generally smaller distance values than the heme-metal-center metric. Nevertheless, there is noticeable spread of the data to the left and right of the best fit lines, which may well reflect poor distance estimates due to range of motion. Fig. 3A, which uses the Ru-to-macrocycle metric, shows that depending on the particular Ru label, this possible range of motion can be quite large. One way to avoid this issue is to remove from consideration those points with the greatest mobility, including only those that have a range of motion of 2 Å or less, and are thus likely to introduce a less than a 16-fold change in tunneling rate. Fig. 3B, which shows the restricted data set with better defined distances without a wide range of motion, reveals a best fit to this data set that is remarkably similar to that seen for the edge-to-edge distances in photosynthetic reaction centers (Fig. 3C). This suggests there is a consistent tunneling distance metric that includes the porphyrin macrocycle edge of both hemes and chlorins.

We have compared distance metrics measured from the metal of the Ru center to the heme iron or macrocycle edge. It is of course possible to choose alternative distance metrics for the Ru center itself, such as the distance from atoms liganding the Ru, or from the edge of the pyridyl rings. We find the best working definition of the "edge" of a redox center for estimating electron-tunneling rates using Eq. (1)

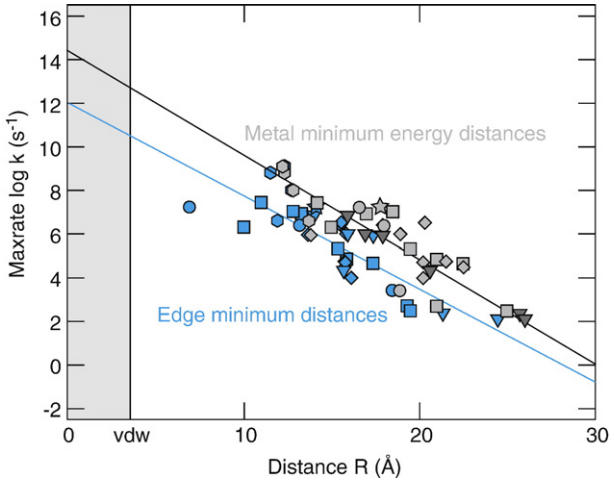

Fig. 2. Free energy optimized electron-tunneling rates with different distance metrics. Blue: electron-transfer distances defined as Ru metal-to-heme edge with Ru label position at minimum distance; gray: Ru metal-to-Fe metal at likely Ru label position estimated by Gray[16]. Ruthenated heme proteins include myoglobin[10,11,37] (circles), *cyt c*[11–18,38–40] (diamonds), *cyt* b_5[19,20] (star) and *cyt* b_{562}[16] (squares). Also included for comparison are ruthenated azurins[10,22,23], a copper protein (triangles) and HiPIP, an iron-sulfur protein (hexagons)[24].

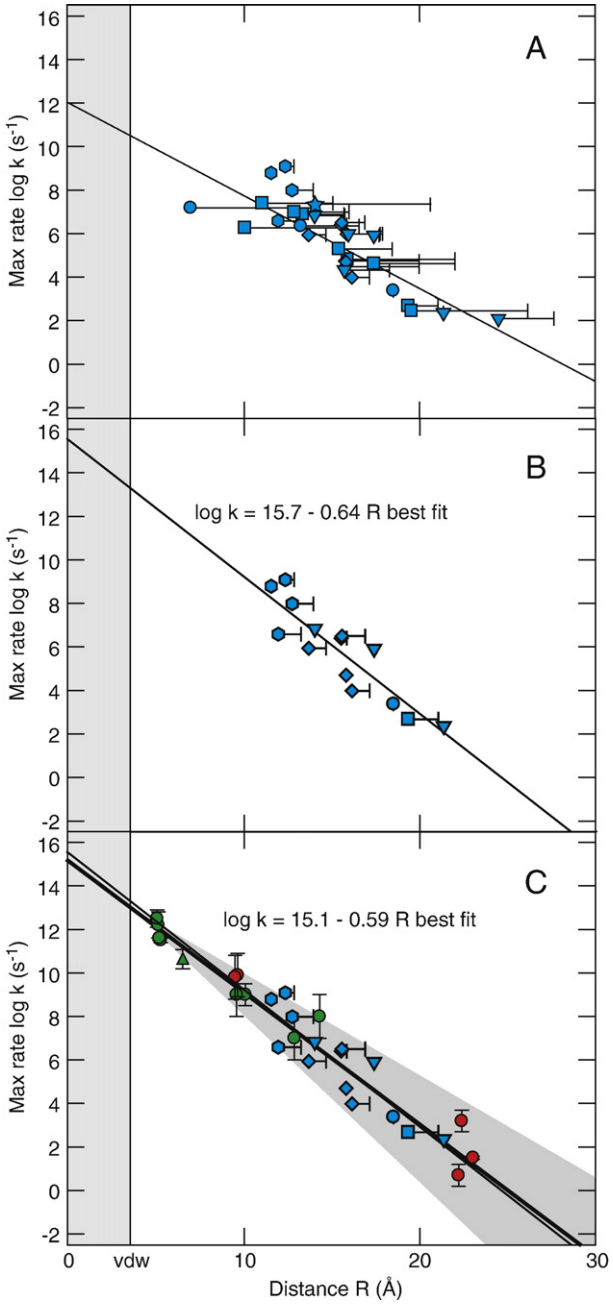

Fig. 3. Distance/rate dependence of ruthenated proteins. A) Ru-heme edge minimum distances showing possible range of movement. B) Subset with range of movement less than 2 Å. C) Comparison of this subset with bacterial RC and PSI rates.

to be the metal itself for ruthenium and copper centers, the iron and sulfurs bound between irons for iron- sulfur clusters, and the porphyrin macrocycle for hemes. These are the distances plotted in the figures. When the non-heme cofactors are expanded to include the other atoms ligated to the metal, the electron-tunneling rates are overestimated as a group by more than an order of magnitude.

1.3. Molecular dynamics estimates of distances and heme axial tunneling

Rather than choose a distance metric based on an energy minimized structure model or a minimum distance model as just described, it is possible to perform a more sophisticated molecular dynamics simulation[25] on each Ru labeled variant and consider this dynamic effect on electron-tunneling distances. This has recently been done for the Ru centers for the cytochromes *c* and b_{562}[9] in an

analysis of the electron-tunneling rates. In this work, the movement of the Ru labeled variants was modeled using molecular dynamics on the 100 ps timescale and the electronic coupling between the donor and acceptor sites were computed for each 1 ps geometric snapshot. This dynamical simulation led to a set of metal-to-metal distances that were only slightly different from the energy minimized distances reported by Gray[16] (Fig. 4A).

Prytkova et al. noted that three of these points (two *cyt* b_{562} and one *cyt c*) did not appear to be in the same cluster as the others[9]. They observed that these points have relatively shorter distances and lower rates, and share the property of a nearly axial geometry between the heme plane and the Ru label position, with best linkage paths between donor and acceptor arriving via the heme axial ligand. The conclusion was drawn that because axial orientation tends to have one dominant best path compared to more edge-on geometries (which tend to have several comparably linked paths), there was an opportunity for axial geometries to have unusually well-coupled or poorly-coupled links for a given metal-to-metal distance, and less opportunity for averaging interference between multiple paths. These three points happened to all have depressed rates relative to the main group of ruthenated protein data, but Prytkova anticipated that enhanced rates would be found if more axially coupled examples were examined[9].

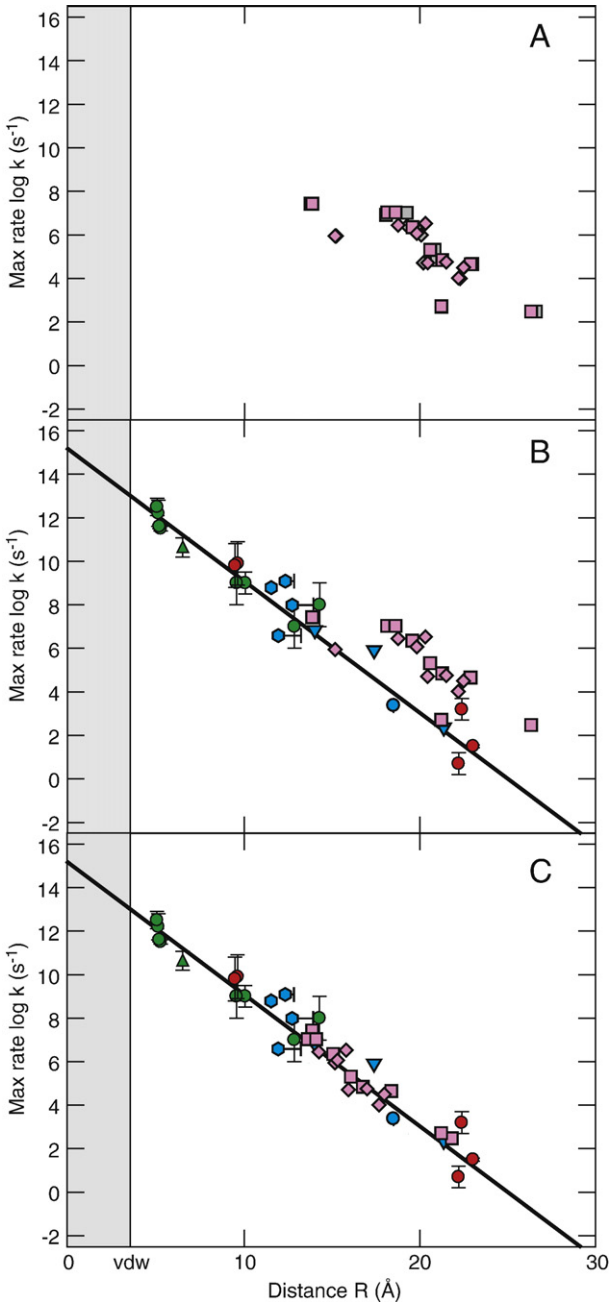

Fig. 4. Free energy optimized tunneling rates using molecular dynamics defined distances. A) Comparison of the Ru–Fe tunneling distances for *cyt c* and b_{562} estimated by energy minimization (gray) or molecular dynamics (pink). B, C) Comparison of Ru to Fe molecular dynamics distances with RC edge-to-edge (green, red) and Ru to heme edge-to-edge minimum distances (blue) for subset with <2 Å variance in distance. Panel B includes the unadjusted metal-to-metal distances, and panel C includes the same distances minus a 4.8 Å heme diameter in order to estimate the heme-to-macrocycle edge distance for this molecular dynamics data set.

The metal-to-macrocycle metric suggests an alternative explanation and a different prediction for rates of future measurements of heme axially-oriented electron- transfer reactions. Fig. 4B shows that if these metal-to-metal distances for ruthenated cytochrome *c* and b_{562} are adjusted to metal-to-macrocycle distances and plotted together with metal-to-macrocycle rates and distances for other ruthenated proteins and the edge-to-edge rates and distances of reaction centers of Fig. 3C, these three axial examples become unremarkable and fall within the same grouping with rates well predicted by the simple empirical Eq. (1). Only one of the myoglobin ruthenium labels so far has a distance variance of less than 2 Å and is included in Fig. 4B; this has an axial orientation and is also unremarkable. Edge-oriented Ru-heme electron transfers fall at lengthy distances only when the metal-to-metal distance metric is used. Indeed, applying a rough correction to this edge-oriented set by subtracting half a heme diameter (4.8 Å) brings the seemingly errant majority of ruthenated observations back into the general intraprotein electron-transfer group (Fig. 4C). Using the metal-to-macrocycle metric as opposed to the metal-to-metal metric means that there is no requirement for exceptionally good or poor coupling between redox cofactors, or a need for averaging interference effects to distinguish axial from edge coupling, at least within the approximately order of magnitude experimental error introduced by uncertainties in rates, distances, driving force and reorganization energy. We predict that when using the metal-to-metal distance metric, future observed rates for axial heme pathway geometries will generally be lower than the analogous edge-on geometries, simply because the metal-to-metal metric tends to overestimate the effective tunneling distances for the edge- geometries by up to half a heme diameter.

1.4. Heme/metal distance metrics in other natural heme electron transfers

There are nearly a dozen natural heme electron-transfer reactions for which crystal structure distances are available and electron-transfer rates and driving forces have been measured, but their reorganization energies have not been particularly well determined. This unknown reorganization energy leads to uncertainty in the estimate of the free energy optimized electron-tunneling rate. Nevertheless, it is useful to examine these natural heme electron-transfer reactions, assuming either generic reorganization energy values or reported values based on the temperature dependence of the reaction, in order to make a rough comparison of the heme-metal vs. heme-edge distance metrics. Fig. 5A and B show the heme-metal and the heme-edge metrics respectively overlaid on the data of Fig. 4B and C, using default heme electron-transfer reorganization energies of 1 eV unless otherwise reported. It is clear that even with these substantial uncertainties in estimating free energy optimized rates, the heme-edge distance metric of Fig. 5B falls in the same grouping as the other heme-edge metrics, with an average deviation less than an order of magnitude from the original best fit line drawn for the photosynthetic reaction center data points. The generic square barrier model of Eq. (1) represents a fair estimate of observed reaction rate for this expanded set of heme reactions provided electron-tunneling distances use the

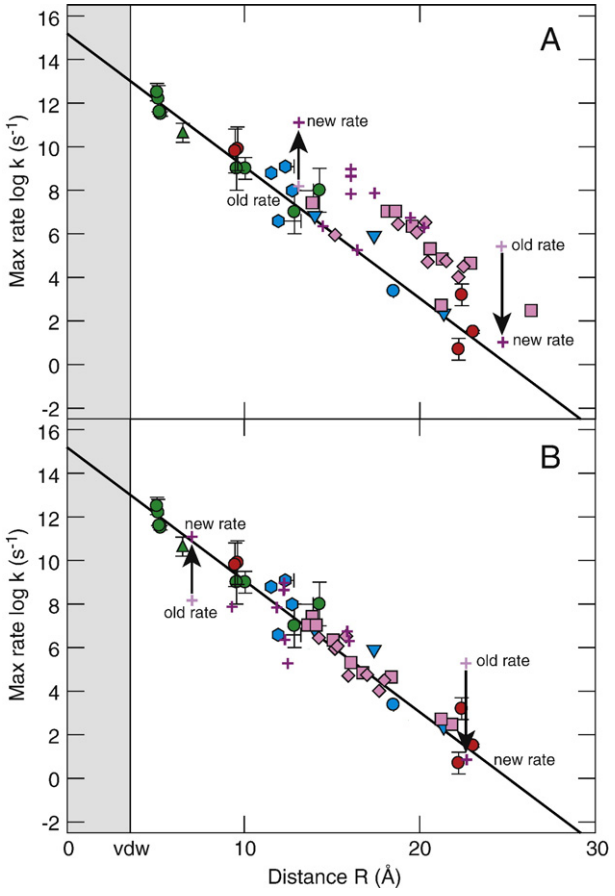

Fig. 5. A comparison of heme-metal and heme-edge metrics. In addition to Ru-heme and photosynthetic electron transfers, natural heme electron transfers with estimated reorganization energies (purple crosses) are plotted with either a heme-metal distance metric (A) or a heme-edge distance metric (B). These reactions include heme to $BChl_2$ in *Rps. viridis* photosynthetic reaction centers[41,42], cytochrome oxidase heme *a* with heme a_3 [31] and Cu_A [43], heme b_L to b_H [44] and heme c_2 to c_1 in cytochrome bc_1 [45,46], heme to tryptophan in cytochrome *c* peroxidase[47], Cu to heme in methylamine dehydrogenase[26] and heme to 3Fe4S in fumarate reductase[48,49]. Original measurements of heme electron-transfer rates for cytochrome oxidase and methylamine dehydrogenase that were far from the simple square barrier line have since been remeasured and now fall close to the line (arrows).

heme macrocycle as the definition of the cofactor edge, as would be expected if the wavefunction for an electron on a heme can be treated as relatively delocalized over the heme porphyrin macrocycle, with a much steeper, approximately exponential decay of the wavefunction once it passes beyond this heme edge.

1.5. Medium effects in heme/heme electron tunneling

Two of the heme reactions in this expanded data set deserve particular attention because the original rate measurements were orders of magnitude different from the rates predicted by a square barrier model. They were cited as examples of failure of that model and successes for medium dependent pathway models, which appeared to predict rates correctly. It was only later when new measurements changed these rate values by several orders of magnitude that it became clear that the simple square barrier model had indeed predicted rates correctly after all.

The long-distance reaction of copper to heme in methylamine dehydrogenase[26] had a measured rate in solution four orders of magnitude faster than predicted by a simple, generic square barrier model. Such a large deviation is exactly what would be expected for an exceptionally well-coupled pathway[27] that has been selected by Nature to speed this useful, long-distance electron-transfer reaction. Indeed, the relatively fast rate in solution was shown to be consistent with the long electron-transfer distance in the crystal structure of the complex when a pathway analysis was performed[26,28].

However, when electron-transfer rates in the crystals themselves were measured[29], a completely different picture emerged: copper to heme electron-transfer rates are nearly 4 orders of magnitude slower in crystals than they are in solution, and therefore, now entirely consistent with a generic tunneling barrier. In addition, mutational changes of the medium between the copper and heme centers that were expected to disrupt the pathways and dramatically alter electron-transfer rates showed no effect[28].

A complementary example is provided by the heme *a* to a_3 electron transfer in cytochrome oxidase, which was also cited as a failure of the square barrier model and the success of a pathway model [30]. The originally accepted experimental rate was approximately a thousand times slower than expected for a generic square barrier model. Pathway calculations at that time were used to show that the coupling was exceptionally poor for the short distance, and used to explain the slow rate[30]. New experiments increased the rate for the cytochrome oxidase reaction to a few nanoseconds[31], close to the value predicted by the square barrier model[4,32]. The pathway analysis was repeated using dynamics and quantum interference effects[33] to yield a rate more consistent with the new measurement.

Perhaps it should not come as much of a surprise that with such a short heme edge-to-edge electron-tunneling distance between *a* to a_3 that the measured rate falls close to the square barrier line. The 7 Å edge-to-edge distance between hemes is just 3.4 Å longer than the van der Waals contact. While estimates of packing densities at such short distances are more uncertain, as mentioned in a recent report [34], the effect of these uncertainties in packing density is muted by the short distance the electron tunnels through the insulating protein medium. Even cutting the packing density drastically to half of the typical protein value would only slow the expected *a* to a_3 tunneling rate by 10-fold. The restricted effect of tunneling medium changes over short tunneling distances makes it unlikely that natural selection can apply much pressure here. Rather, the principal engineering of the *a* to a_3 electron transfer near the catalytic site of cytochrome oxidase appears to be blunt and simple: keep electron-tunneling distances short and the inherent electron-tunneling rates fast, so that the penalty associated with surmounting large, Eyring-style chemical activation energy barriers at the catalytic site can be overcome in milliseconds or faster[32].

While natural selection of the protein tunneling medium remains a possibility, so far, it does not appear that there are any clear examples in which the protein medium has been selected by Nature to modulate the electron-tunneling barrier by speeding up physiologically useful electron-transfer reactions or slowing down physiologically unproductive ones. Instead, natural engineering of electron tunneling seems prosaic, guiding electron transfer through multi-cofactor proteins by favoring designs that place productive redox centers closer together and keep unproductive, short-circuiting redox partners further apart.

2. Conclusion

When ruthenated heme protein data were examined according to a metal-to-metal metric[9], 4 out of 20 examples fell two orders of magnitude below the rate vs. distance trend expected for a simple square barrier tunneling model. This prompted an explanation in terms of pathway tunneling calculations which allowed quantum interference effects between paths. The results presented here show that when the same data are examined using a metal-to-macrocycle metric, these 4 points join the rest of the ensemble. This indicates that a simple square barrier tunneling model remains an adequate description of protein electron tunneling, within experimental error, for a variety of cofactors, including chlorins, quinones, ruthenium centers, and hemes. Although the tunneling wavefunction is not

spread uniformly over the heme any more than it is for the other cofactors, it will be spread much more evenly than an exponential decay with distance from the central iron, which makes the macrocycle edge description a practical one. Further, we predict that axially-oriented heme electron transfers will systematically appear slow compared to non-axial, more edge-oriented electron transfers in metal-to-metal metrics, simply because the edge orientations will benefit from the spread of the electron wavefunction over the heme towards the donor or acceptor. This prediction stands in contrast to a pathway interference description[9], which anticipates that axial orientations may be either faster or slower than edge orientations for a given heme-metal distance.

Acknowledgments

Supported by grants from DOE DE-FG02-05ER46223, NIH GM48130, and a NSF Graduate Student Fellowship.

References

[1] C.C. Page, C.C. Moser, X.X. Chen, P.L. Dutton, Natural engineering principles of electron tunnelling in biological oxidation-reduction, Nature 402 (1999) 47–52.
[2] R.A. Marcus, N. Sutin, Electron transfers in chemistry and biology, Biochim. Biophys. Acta 811 (1985) 265–322.
[3] M.R. Gunner, P.L. Dutton, Temperature and Delta-G-Degrees dependence of the electron-transfer from Bph.- to Qa in reaction center protein from Rhodobacter-Sphaeroides with Different Quinones As Qa, J. Am. Chem. Soc. 111 (1989) 3400–3412.
[4] C.C. Moser, J.M. Keske, K. Warncke, R.S. Farid, P.L. Dutton, Nature of biological electron-transfer, Nature 355 (1992) 796–802.
[5] M. Iwaki, S. Kumazaki, K. Yoshihara, T. Erabi, S. Itoh, Delta G(0) dependence of the electron transfer rate in the photosynthetic reaction center of plant photosystem I: natural optimization of reaction between chlorophyll a (A(0)) and quinone, J. Phys. Chem. 100 (1996) 10802–10809.
[6] S. Itoh, M. Iwaki, I. Ikegami, Modification of photosystem I reaction center by the extraction and exchange of chlorophylls and quinones, Biochim. Biophys. Acta 1507 (2001) 115–138.
[7] C.C. Page, C.C. Moser, P.L. Dutton, Mechanism for electron transfer within and between proteins, Curr. Opin. Chem. Biol. 7 (2003) 1–6.
[8] I.A. Balabin, J.N. Onuchic, Dynamically controlled protein tunneling paths in photosynthetic reaction centers, Science 290 (2000) 114–117.
[9] T.R. Prytkova, I.V. Kurnikov, D.N. Beratan, Coupling coherence distinguishes structure sensitivity in protein electron transfer, Science 315 (2007) 622–625.
[10] H.B. Gray, J.R. Winkler, Electron transfer in proteins, Annu. Rev. Biochem. 65 (1996) 537–561.
[11] H.B. Gray, J.R. Winkler, Electron tunneling through proteins, Q. Rev. Biophys. 36 (2003) 341–372.
[12] D.N. Beratan, J.N. Onuchic, J.R. Winkler, H.B. Gray, Electron-tunneling pathways in proteins, Science 258 (1992) 1740–1741.
[13] B.E. Bowler, T.J. Meade, S.L. Mayo, J.H. Richards, H.B. Gray, Long-range electron transfer in structurally engineered pentaammineruthenium (histidine-62) cytochrome *c*, J. Am. Chem. Soc. 111 (1989) 8757–8759.
[14] M.J. Therien, M. Selman, H.B. Gray, I.J. Chang, J.R. Winkler, Long-range electron transfer in ruthenium-modified cytochrome c: evaluation of prophyrin-ruthenium electronic couplings in the *Candida krusei* and horse heart proteins, J. Am. Chem. Soc. 112 (1990) 2420–2422.
[15] M.J. Therien, J. Chang, A.L. Raphael, B.E. Bowler, H.B. Gray, Long-range electron-transfer in metalloproteins, Struct. Bond. 75 (1991) 109–129.
[16] J.R. Winkler, A.J. Di Bilio, N.A. Farrow, J.H. Richards, H.B. Gray, Electron tunneling in biological molecules, Pure Appl. Chem. 71 (1999) 17531764.
[17] D.S. Wuttke, H.B. Gray, S.L. Fisher, B. Imperiali, Semisynthesis of bipyridyl-alanine cytochrome c mutants: novel proteins with enhanced electron transfer properties, J. Am. Chem. Soc. 115 (1993) 8455–8456.
[18] D.R. Casimiro, J.H. Richards, J.R. Winkler, H.B. Gray, Electron-transfer in ruthenium-modified cytochromes-*c*-sigma-tunneling pathways through aromatic residues, J. Phys. Chem. 97 (1993) 13073–13077.
[19] J.R. Scott, A. Willie, M. McLean, P.S. Stayton, S.G. Sligar, B. Durham, F. Millett, Intramolecular electron-transfer in cytochrome-*b*(5) labeled with ruthenium(II) polypyridine complexes-rte measurements in the Marcus inverted region. J. Am. Chem. Soc. 115 (1993) 6820–6824.
[20] A. Willie, P.S. Stayton, S.G. Sligar, B. Durham, F. Millett, Genetic engineering of redox donor sites: measurement of intracomplex electron transfer between ruthenium-65-cytochrome b5 and cytochrome c, Biochemistry 31 (1992) 7237–7242.
[21] M.J. Bjerrum, D.R. Casimiro, I.-J. Chang, A.J. Di Bilio, H.B. Gray, M.G. Hill, R. Langen, G.A. Mines, L.K. Skov, J.R. Winkler, D.S. Wuttke, Electron transfer in ruthenium modified proteins, J. Bioenerg. Biomembr. 27 (1995) 295–302.
[22] R. Langen, I.J. Chang, J.P. Germanas, J.H. Richards, J.R. Winkler, H.B. Gray, Electron tunneling in proteins: coupling through a beta strand, Science 268 (1995) 1733–1735.
[23] A.J. DiBilio, M.G. Hill, N. Bonander, B.G. Karlsson, R.M. Villahermosa, B.G. Malmstrom, J.R. Winkler, H.B. Gray, Reorganization energy of blue copper: Effects of temperature and driving force on the rates of electron transfer in ruthenium- and osmium-modified azurins, J. Am. Chem. Soc. 119 (1997) 9921–9922.
[24] E. Babini, I. Bertini, M. Borsari, F. Capozzi, C. Luchinat, X.Y. Zhang, G.L.C. Moura, I.V. Kurnikov, D.N. Beratan, A. Ponce, A.J. Di Bilio, J.R. Winkler, H.B. Gray, Bond-mediated electron tunneling in ruthenium-modified high-potential iron-sulfur protein, J. Am. Chem. Soc. 122 (2000) 4532–4533.
[25] S.S. Skourtis, I.A. Balabin, T. Kawatsu, D.N. Beratan, Protein dynamics and electron transfer electronic decoherence and non-Condon effects, Proc. Natl. Acad. Sci. U. S. A. 102 (2005) 3552–3557.
[26] V.L. Davidson, L.H. Jones, Electron transfer from copper to heme within the methylamine dehydrogenase-amicyanin-cytochrome *c*-551i complex, Biochemistry 35 (1996) 8120–8125.
[27] J.J. Regan, S.M. Risser, D.N. Beratan, J.N. Onuchic, Protein electron transport: single vs multiple pathways, J. Phys. Chem. 97 (1993) 13083–13088.
[28] V.L. Davidson, L.H. Jones, E. Graichen, Z. Zhu, Tyr-30 of amicyanin is not critical for electron transfer to cytochrome *c*-551i: implications for predicting electron transfer pathways, Biochim. Biophys. Acta 1457 (2000) 27–35.
[29] D. Ferrari, A. Merli, A. Peracchi, M. Di Valentin, D. Carbonera, G.L. Rossi, Catalysis and electron transfer in protein crystals: the binary and ternary complexes of methylamine dehydrogenase with electron acceptors, Biochim. Biophys. Acta 1647 (2003) 337–342.
[30] J.J. Regan, B.E. Ramirez, J.R. Winkler, H.B. Gray, B.G. Malmstrom, Pathways for electron tunneling in cytochrome c oxidase, J. Bioenerg. Biomembr. 30 (1998) 35–39.
[31] M.I. Verkhovsky, A. Jasaitis, M. Wikstrom, Ultrafast haem–haem electron transfer in cytochrome c oxidase, Biochim. Biophys. Acta 1506 (2001) 143–146.
[32] C.C. Moser, C.C. Page, P.L. Dutton, Darwin at the molecular scale: selection and variance in electron tunneling proteins including cytochrome c oxidase, Phil. Trans. Roy. Soc. B 361 (2006) 1295–1305.
[33] M.-L. Tan, I.A. Balabin, J.N. Onuchic, Dynamics of electron transfer pathways in cytochrome c oxidase, Biophys. J. 86 (2004) 1813–1819.
[34] A. Jasaitis, M.P. Johansson, M. Wikstrom, M.H. Vos, M.I. Verkhovsky, Nanosecond electron tunneling between the hemes in cytochrome bo3, Proc. Natl. Acad. Sci. U. S. A. 104 (2007) 20811–20814.
[35] J. Deisenhofer, O. Epp, H. Sinning, H. Michel, Crystallographic refinement at 2.3 Å resolution and refined model of the photosynthetic reaction centre from *Rhodopseudomonas viridis*, J. Mol. Biol. 246 (1995) 429–457.
[36] P. Jordan, P. Fromme, H.T. Witt, O. Klukas, W. Saenger, N. Krauss, Three-dimensional structure of cyanobacterial photosystem I at 2.5 angstrom resolution, Nature 411 (2001) 909–917.
[37] D.R. Casimiro, D.N. Beratan, J.N. Onuchic, J.R. Winkler, H.B. Gray, Donor-acceptor electronic coupling in ruthenium-modified heme proteins, Adv. Chem. Ser. 246 (1995) 471–485.
[38] I.-J. Chang, H.B. Gray, J.R. Winkler, High-driving force electron-transfer in metalloproteins — intramolecular oxidation of ferrocytochrome-*c* by Ru(2,2'-Bpy)2(Im)(His33)3+, J. Am. Chem. Soc. 113 (1991) 7056–7057.
[39] T.B. Karpishin, M.W. Grinstaff, S. Komarpanicucci, Electron-transfer in cytochrome-*c* depends upon the structure of the intervening medium, Structure 2 (1994) 415–422.
[40] D.R. Casimiro, J.H. Richards, J.R. Winkler, Electron-transfer in ruthenium-modifed cytochromes-*c* — sigma-tunneling pathways through aromatic residues, J. Phys. Chem. 97 (1993) 13073–13077.
[41] R.J. Shopes, L.M.A. Levine, D. Holten, C.A. Wraight, Kinetics of oxidation of the bound cytochromes in reaction centers from *Rhodopseudomonas viridis*, Photosynth. Res. 12 (1987) 165–180.
[42] B. Dohse, P. Mathis, J. Wachtveitl, E. Laussermair, S. Iwata, H. Michel, D. Oesterhelt, Electron-transfer from the tetraheme cytochrome to the special pair in the rhodopseudomonas-viridis reaction-center — effect of mutations of tyrosine L162, Biochemistry 34 (1995) 11335–11343.
[43] D. Zaslavsky, R.C. Sadoski, K.F. Wang, B. Durham, R.B. Gennis, F. Millett, Single electron reduction of cytochrome c oxidase compound F: resolution of partial steps by transient spectroscopy, Biochemistry 37 (1998) 14910–14916.
[44] V.P. Shinkarev, A.R. Crofts, C.A. Wraight, The electric field generated by photosynthetic reaction center induces rapid reversed electron transfer in the bc(1) complex, Biochemistry 40 (2001) 12584–12590.
[45] H. Tian, R. Sadoski, L. Zhang, C.A. Yu, L. Yu, B. Durham, F. Millett, Definition of the interaction domain for cytochrome *c* on the cytochrome *bc*(1) complex — steady-state and rapid kinetic analysis of electron transfer between cytochrome *c* and *Rhodobacter sphaeroides* cytochrome *bc*1 surface mutants, J. Biol. Chem. 275 (2000) 9587–9595.
[46] C. Lange, C. Hunte, Crystal structure of the yeast cytochrome *bc*(1) complex with its bound substrate cytochrome *c*, Proc. Natl. Acad. Sci. U. S. A. 99 (2002) 2800–2805.
[47] H.K. Mei, K.F. Wang, N. Peffer, G. Weatherly, D.S. Cohen, M. Miller, G. Pielak, B. Durham, F. Millett, Role of configurational gating in intracomplex electron transfer from cytochrome c to the radical cation in cytochrome c peroxidase, Biochemistry 38 (1999) 6846–6854.
[48] C.R.D. Lancaster, *Wolinella succinogenes* quinol: fumarate reductase — 2.2-A resolution crystal structure and the E-pathway hypothesis of coupled transmembrane proton and electron transfer, Biochim. Biophys. Acta 1565 (2002) 215–231.
[49] A. Kroger, S. Biel, J. Simon, R. Gross, G. Unden, C.R.D. Lancaster, Fumarate respiration of *Wolinella succinogenes*: enzymology, energetics and coupling mechanism, Biochim. Biophys. Acta 1553 (2002) 23–38.